

Characterization and measurement of gamma radiation shielding of a new tungsten-lignin composite

Journal of Composite Materials
2021, Vol. 55(24) 3579–3588
© The Author(s) 2021
Article reuse guidelines:
sagepub.com/journals-permissions
DOI: 10.1177/00219983211029364
journals.sagepub.com/home/jcm



Armando Cirilo de Souza¹, Flavio Aristone² ,
Adriana Fatima Gomes Gouvea¹, Hedielly Brasil Fernandes¹,
Adailto Miyai² and Jesualdo Rossi³

Abstract

This research has been carried on to analyze the capability of a new composite to be effectively used as shielding of gamma radiation. The preparation of a metal-organic composite formed by tungsten and Kraft lignin is presented. Samples have been characterized through X-rays and scanning electron microscopy measurements. The results led to the study of the different phase formations. The microscopic analyzes indicate that two different phases are present in the composite. The absence of oxidation in the process even after the temperature treatment imposed to form the sample has also been noticed. Measurements of the attenuation have been performed to study its ability to absorb gamma radiation. A sample of cobalt 60 (Co-60), for which the peak energies are at 1173 keV and 1332 keV, was used as a source of gamma radiation in the experiment of attenuation. The measured attenuation of gamma radiations when the composite is placed to act as a shield is only 16% smaller than the attenuation obtained for standard pure tungsten. This is a clear indication that the new metal-organic composite is suitable for the fabrication of devices dedicated to shielding radiation, with the advantage of being easier to manipulate.

Keywords

Composite, lignin-tungsten, gamma radiation, characterization, shielding effect

Introduction

The current demand for new materials appropriate to be used as a shield of radiation is consistently growing. There is a particular interest in the research of those materials suitable for the transportation of radiopharmaceutical products used, e.g., in the diagnosis of cancer and cancer therapies.¹

Tungsten is widely used in the nuclear sector, as it possesses large mechanical resistance and an excellent working cross-section on the attenuation of thermal neutrons.² Nevertheless, it is interesting to search for new composites involving tungsten and other materials for technological purposes due to practical reasons.³ The idea of mixing standard tungsten with organic materials to form composites is particularly interesting due to the possibility of obtaining new materials easier to manipulate and suitable to be used as radiation shields.⁴

The phenomenon of radiation attenuation occurs through the processes of absorption and/or dispersion

of given particles or photon energies when they interact with atoms of the target material.⁴ The characteristics of the shielding effect are directly linked to the scattering cross-section of each material, which can be attributed to its atomic density.⁵ From that perspective, standard tungsten is particularly efficient.³ Nevertheless, the construction of certain types of equipment such as, e.g., recipients destined for the transportation of radioactive materials, demands new

¹Department of Physics – CEPEMAT, State University of South Mato Grosso, Dourados – MS, Brazil

²INFI – Federal University of South Mato Grosso, Campo Grande – MS, Brazil

³IPEN – Av. Prof. Lineu Prestes, São Paulo-SP, Brazil

Corresponding author:

Flavio Aristone, Federal University of South Mato Grosso, Avenida Costa e Silva, Campo Grande 79070-900, Brazil.

Email: flavio.aristone@ufms.br

materials easier to process and manipulate, even if small losses on the effectiveness of the shielding capacity occur.⁶

Kraft lignin and powder tungsten have been mixed and properly manipulated to originate a new metal-organic composite more malleable than the pure standard metal. After processing samples, they have been characterized with the help of scanning electron microscopy (SEM) and X-ray diffraction (XRD) measurements.⁷ Samples sintered at different temperatures have been characterized to help the study of the composite formation and determine its optimal manipulation conditions.

The experimental setup used to obtain these samples is described in the next section. Typical results of SEM and XRD are exhibited and studied to help the physical characterization of this composite. Measurements of the transmission of gamma radiation passing thru the new composite used as a shield are compared to equivalent results obtained for standard tungsten. The shielding coefficient of both materials is obtained and compared in the final part of this paper. The present results led to conclusions about the shielding effectiveness of the new composite. The sintering of lignin and tungsten to forming a composite originated a new material suitable for pieces of equipment destined for transportation of radioactive materials.⁸ The new composite is only 16% less effective than pure tungsten but considerably easier to be handled.

Materials and methods

Powder of pure metallic tungsten and Kraft lignin have been mixed, pressed, and sintered to form a new composite. The concentration of tungsten and lignin were varied, originating a series of different samples to be studied. However, the present results discussed in this paper have been obtained for a specific case denominated W5Lig, referring to a composite made of 95% tungsten and 5% lignin. The percentage relates to the total composite resulting mass.

The lignin is obtained from the black liquor of the Kraft process in the extraction of cellulosic pulp.⁸ The black Kraft liquor of lignin is removed, then isolated via carbonation, and finally acidified up to a pH 2.

Carbonic gas is bubbled into the black liquor until approximately 75% - 80% of lignin be recovered by direct filtration. The resulting filtrate is treated with sulfuric acid. Afterward, approximately 10% of the Kraft lignin is recovered as a powder.⁸ The schematic process is represented in Figure 1.

The lignin powder obtained shall be mixed with tungsten powder, pressed, and sintered to form the composite that will be tested.^{8,9} The detailed process consists of blending lignin and tungsten powders until uniformity is reached. The average size of particles is controlled and limited to 13 μm approximately. This intermediary material is pressed up to a load of 15 tons/cm², originating a raw sample sized 1,2 cm diameter and 0,8 cm tall, exhibited in Figure 2.¹⁰

The heating treatment is the final step of sample preparation, which intends the sintering of the intermediary raw sample. Four samples have been submitted to different temperatures to determine the optimal heating treatment to sinter the composite. The samples 1 thru 4 were heated at 60 °C, 70 °C, 80 °C, and 90 °C, respectively. The heating rate was 10 °C/min for all samples. During the process, each sample has been held at its specific temperature of sintering for one hour. After cooling down to room temperature, they are ready for the sequence of characterizations and test measurements.¹¹ The mix of lignin and tungsten powders must be sintered to form a piece of new material. Therefore, instead of two separated agglomerated powders, they shall originate a single material through



Figure 2. Two intermediary samples of W5Lig, obtained after pressing but before sintering.

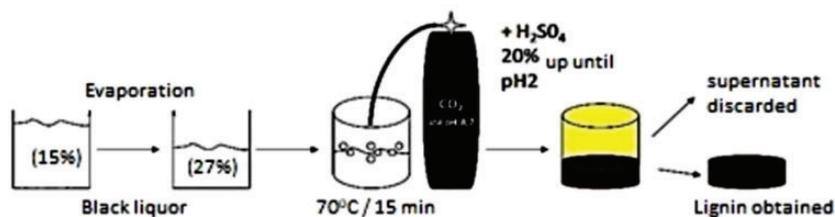


Figure 1. Schematic experimental setup to obtain a powder of Kraft lignin.

agglutination. Lignin is an organic macromolecule formed by different hydroxyls and C-C connections. These characteristics are particular for each wood and region of origin. Different lignin implies different structures.

The composite has been submitted to XRD measurements to determine the different phases co-existing in the sample. A K_{α} Cu with λ in the 1.54056 Å to 1.54439 Å range was used as a source.¹² The XRD spectrum gives information about the matrix of elements forming the composite.

The sample morphology is characterized with the help of imagery obtained from a Scanning Electron Microscope (SEM) equipped with Energy Dispersive X-ray Spectroscopy (EDS). Information like sample homogeneity, grain size dispersion, and the precise amount of tungsten and lignin forming the sample are extracted from these images or micrographs.¹³

Finally, the composite obtained is tested to evaluate its capability to attenuate gamma radiation when used as a shield. In fact, this analysis is the ultimate goal of such a study, to compare the shielding effect of the composite to the attenuation from standard tungsten. The experiment consists of measuring the attenuation of gamma radiation sent to pass thru samples of pure tungsten or thru the composite. The experimental setup is showed in Figure 3. A sample of cobalt 60 (Co-60) is used as the source of gamma radiation. A detector of gamma radiation type MOD.2M/2 BRICRON is positioned after the shield to measure the residual radiation. The computer software used for data acquisition that counts the photons passing thru the samples is coupled to an oscilloscope GW-INSTEK GDS-2062 and a spectroscopic amplifier connected to a high voltage stabilizer TCH 1500-2E.

Results and discussions

The results presented in this paper are divided into three subsections and discussions. The morphological characterization is showed first and indicates the optimal sintering process thru the analysis of the samples heated at different temperatures. In the sequence, the X-ray spectrum of the composite is exhibited to discuss the structural arrangement resulting in the composite. The final part exhibits the attenuation coefficient observed for the composite, comparing it to the value measured for pure tungsten.

The composite is ready after the sintering process. There are no chemical bonds nor reactions between the lignin and tungsten. The only connection between these two elements is physical agglutination. During the heating treatment, the lining passes from phase solid to liquid and penetrates all empty spaces left by the particles of tungsten powder. Liquid lignin works as

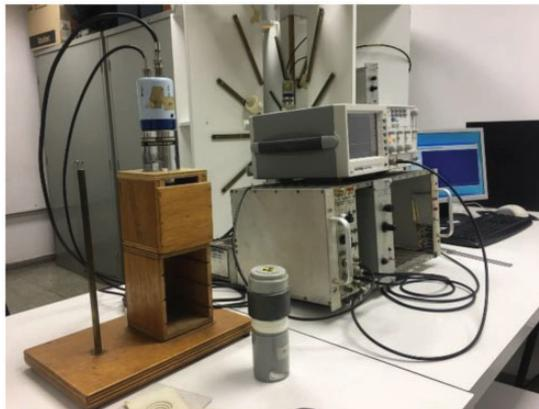


Figure 3. Experimental setup mounted for the detection of gamma radiation.

an adhesive resin agglutinating other particles due to its thermoplastic properties.

Morphological analysis thru scanning electron microscopy

Analysis of micrographs obtained from SEM is important to study the morphological characteristics of sample surfaces. Micrographs of both raw materials have been taken before mixing and sintering them up. The goal is to analyze the intrinsic surface properties of each material individually. Separated micrographs of the two powders used as precursors to form the composite are exhibited in Figures 4 and 5, the Kraft lignin and the pure tungsten, respectively.

Figure 4 shows a typical micrograph of the isolated Kraft lignin powder before mixing it with tungsten to form the composite. This powder is the resulting material obtained after all the steps schematically represented in Figure 1 and described in Materials and methods section. The photograph in Figure 4 shows that the particles on the surface present irregular geometries, and different sizes, certainly for being an organic material. Nevertheless, the resulting granulometry indicates that the average size of particles remains smaller than 10 μm .¹⁴

A typical micrograph of the pure tungsten powder is exhibited in Figure 5. The analysis of granulometry indicates the presence of regular spherical particles around 100 μm in size. All photographs obtained for the tungsten powder used in this study show an excellent overall homogeneity of such a precursor.¹⁴

The next micrograph shows the resulting raw mixture of tungsten and lignin after being pressed at 5 ton/ cm^2 . The sample exhibited in Figure 6 follows the 5:95 proportion for the total mass, i.e., 5% of lignin and 95% of tungsten.¹⁵ It has been named W5Lig. The

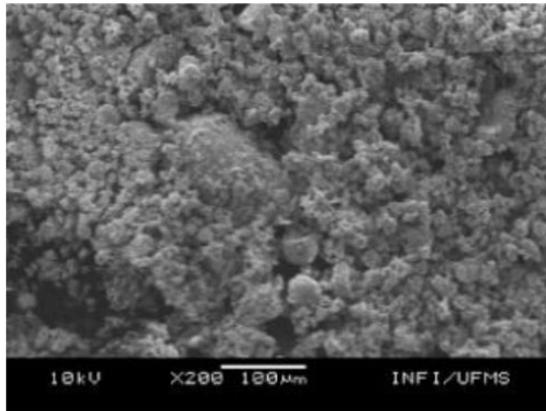


Figure 4. Typical micrograph of the pure Kraft lignin that was used as precursor to form a composite with tungsten.

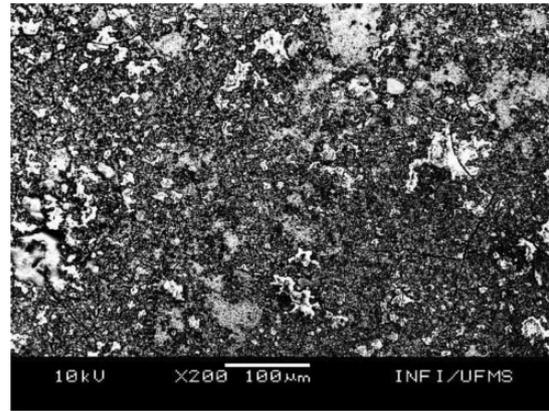


Figure 6. Micrograph of the raw organic-metallic W5Lig mixture pressed at 5 ton/cm².

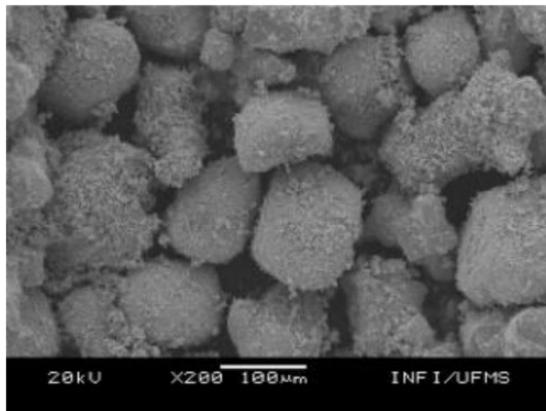


Figure 5. Typical micrograph of the pure standard tungsten powder used as precursor to form the composite with lignin.

concentration of lignin and tungsten are kept constant for all samples analyzed in this paper.

Two different phases are clearly identified in that micrograph, associated with the different brightness of the surface. The brighter parts are associated with tungsten since metallic areas reflect more charges. Conversely, darker areas are attributed to the lignin due to higher concentrations of organic carbon atoms.

The present micrograph is particularly interesting as it gives a clear notion of the role played by the lignin in the composite. It is clear in the figure that the lignin acts as the material agglomerating and connecting the grains of tungsten, originating a solid, steady, and uniform pastille of mixture.¹⁶

The next series of micrographs have been taken after the heating treatment, i.e., when the composite is finished and sintered. As previously described, four different final temperatures of heating have been used to determine the optimal condition of sintering. Therefore, the micrographs exhibited in Figure 7(a)

to (d) are associated with the heating temperatures of 60 °C, 70 °C, 80 °C, and 90 °C, respectively.

These results shall help to determine which temperature generated the best quality sample. Direct visual analysis of these micrographs highlights the effect of different temperatures to reach good sintering. The porosity observed at each micrograph clearly differs from one sample to the next, i.e., from one temperature to the next. As the temperature increases, the porosity decreases due to the higher diffusion of lignin among the grains of tungsten powder.¹⁷ The lignin works as an effective adhesive in the interstices of the tungsten particles.

Higher temperatures facilitate the penetration and equalization of lignin inside the whole pastille. Therefore, higher temperatures result in the improvement of the sample homogeneity. The mechanical resistance of the sample also increases as the sintering temperature increases, even though this result is merely qualitative at this point. Further characterizations regarding this matter are yet to be performed to provide substantial and quantitative arguments.

All the samples shown in Figure 7 have been obtained for the same conditions, except the final temperature of the heating treatment. Therefore, any morphological dissimilarities among these results are due to these differences in temperature.¹⁶

A clear conclusion from these analyses is that the heating temperature of 90 °C presents the best agglutination of the tungsten by the sintered lignin. Nevertheless, when the heating temperature is set above 100 °C, the lignin begins to vitrify, reducing the process of polymerization. Therefore, for temperatures above 100 °C, the sample is no longer isotropic. Therefore, the ideal temperatures for sintering lignin in a matrix of tungsten powder lies between 90 °C and 100 °C.^{16,17}

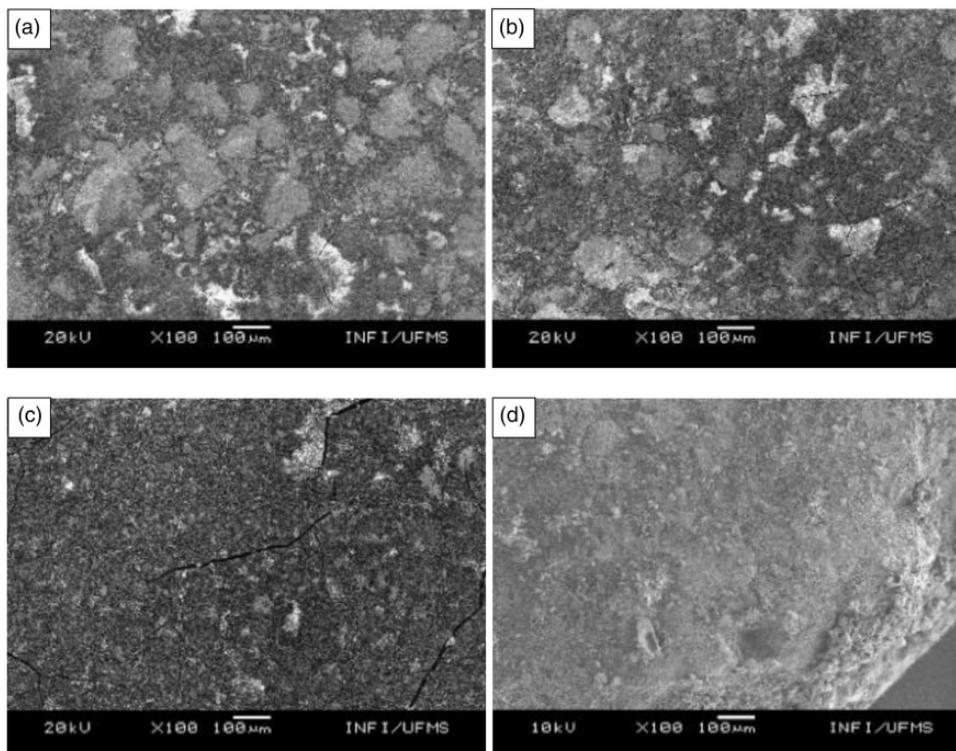


Figure 7. Micrographs obtained for the composite named W5Lig. The final temperatures are: (a) $T = 60^{\circ}\text{C}$; (b) $T = 70^{\circ}\text{C}$; (c) $T = 80^{\circ}\text{C}$; and (d) $T = 90^{\circ}\text{C}$.

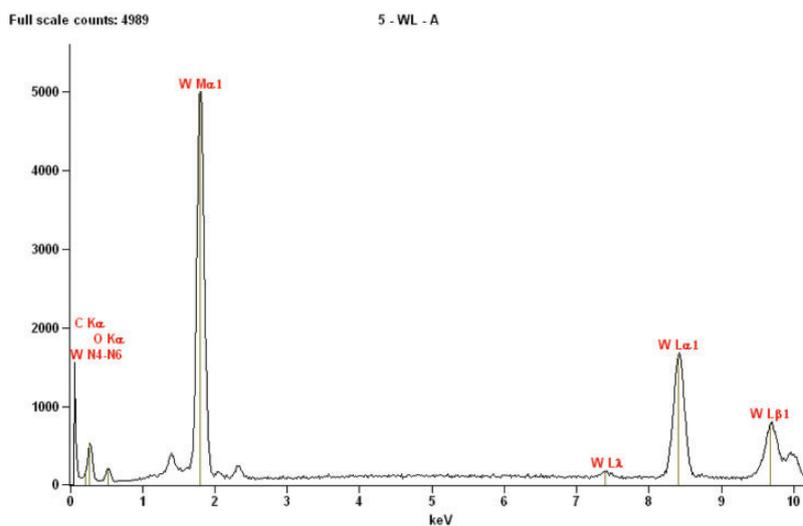


Figure 8. Energy dispersive spectrum obtained for the composite named W5Lig sintered at 90°C .

Characterization thru EDS

The spectrum of energy dispersive spectrum (EDS) obtained for the composite is exhibited in Figure 8. All the results discussed and presented henceforth relate to samples sintered at 90°C . The resulting EDS chart clearly points out every chemical element of the composite, i.e., carbon, tungsten, and oxygen.

As previously mentioned, the final sample is a mixing of 95% of tungsten and 5% of lignin in mass. In the final composite, the carbon responds for 29,39% and the tungsten for 50,73% of the total weight, respectively. The EDS spectrum exhibited is entirely consistent with such a distribution of elements for the composite.¹⁸

Table 1. Values of the masses for the elements present in the composite W5Lig.

Element	Weight %	Weight % error	Atomic %	Atomic % error
C	29.39	±4.04	61.70	±8.49
O	19.88	±1.15	31.34	±1.81
W	50.73	±0.33	6.96	±0.04
Total	100.00		100.00	

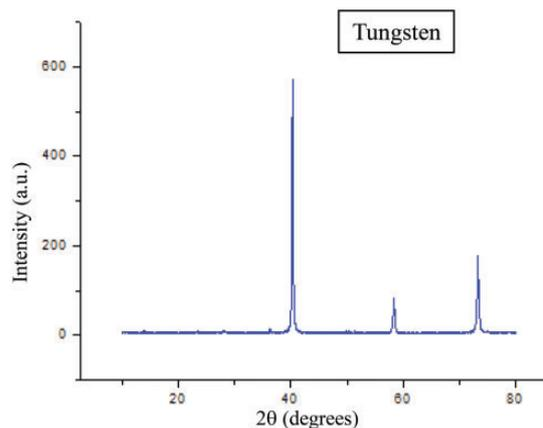
The spectrum in Figure 8 shows the intensity of the signal as a function of the energy provided. The energies characterizing the peaks are associated with the ionization shell of each specific element. The intensity indicates the characteristic transition for each subshell. Four peaks are associated with tungsten, one with carbon, one with oxygen, and one with nitrogen.

Considering the characteristics peaks related to W, the first one (from left to right) corresponds to the ionization of the M shell and consequently an electronic transition to the subshell N to fill the vacancy, represented by α_1 (WM_{α_1}). Although it is a lower energy level, its intensity is higher. The second peak represents the ionization of the L shell with an electronic transition to the subshell O to fill the vacancy, represented by λ (WL_{λ}). The energy, in this case, is higher than the first peak, but it is the lowest intensity of all four.

The third peak represents the ionization of the L shell with an electronic transition from subshell M to fill the vacancy, represented by α_1 (WL_{α_1}). The energy is higher than the two previous transitions, and it is the second-higher intensity of all four. The fourth and last peak for W represents the ionization of the L shell with an electronic transition from subshell N to fill the vacancy, represented by β_1 (WL_{β_1}). It is the highest energy and the third higher intensity of all four peaks.

Both peaks associated with carbon and oxygen correspond to the ionization of the K shell and to the consequent electronic transition of the L subshell to fill the vacancy, represented by α . Both energies are smaller than 0.5 keV. Since there are no electrons in the M shell, only one peak occurs for the carbon. The first peak of the spectrum, represented by WN4N6 in the chart, is also associated with the ionization of the tungsten. In this case, it occurs a lattice relaxation, and consequently an emission closer to the critical energy of N, resulting in X-ray fluorescence.

The spectrum shown in Figure 8 is used to calculate the mass of each element present in the composite. The resulting values are exhibited in Table 1. It was used stoichiometry of mass to mass to assign the missing value to the oxygen that is present in the sample. The missing mass corresponds to 19,88% of the total. The oxygen present in the composite comes from the current C-O-C and C-C interactions in the lignin. They are

**Figure 9.** X-ray spectrum of powder diffraction for the tungsten that was later used as the precursor forming the matrix of the composite.

responsible for the formation of phenolic polymeric chains.

The tungsten and lining densities are 19.25 and 0.457 g/cm³, respectively. The volume of lignin satisfying the stoichiometry is roughly 20 times the tungsten. The carbon and oxygen concentrations measured for the final sample are justified. It is important to mention that the EDS analysis is punctual. Therefore, it is correct to conclude that the agglutination of tungsten powder is due to the concentration of carbon and oxygen present in the lignin.

X-ray diffraction

The X-ray diffraction exhibited in Figure 9 was obtained for the powder tungsten, which later has been mixed with lignin to generate the composite. The resulting chart is typical of the body cubic-centered (BCC) crystal structure. The sharp and neat peaks area piece of clear evidence that the material is very pure.

The measure of the peak positions from the X-ray chart led to the determination of the Miller indices, which classify the possible reflections in the periodic lattice. These indices are used to determine the distances separating periodic plans of the lattice structure. Finally, application of Bragg's law determines the lattice parameters.

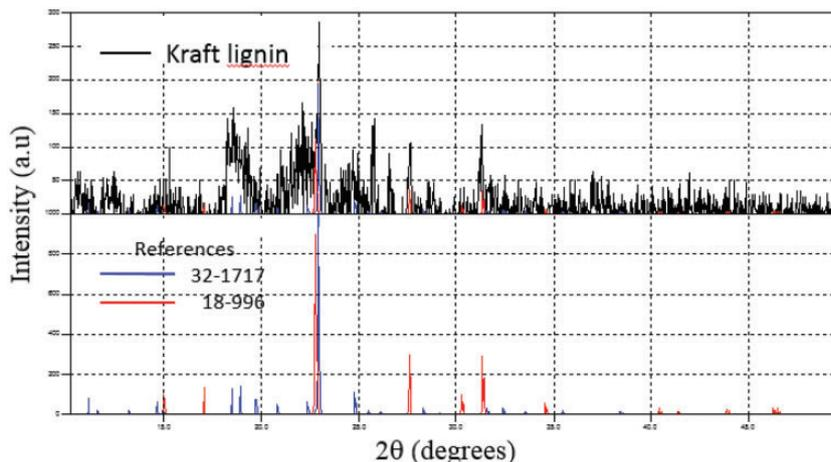


Figure 10. Top: XRD of the pure lignin that will be mixed with tungsten. Bottom: Spectra extracted from the literature for materials 32-1717 and 18-996.

Two spectra are exhibited in Figure 10. The first one at the top has been obtained for the lignin alone after it was extracted and completely dried. The spectrum of the lignin is completely white, i.e., there is no dominant periodic structure prevailing inside the sample. These results are in agreement with all expectations, it is a typical spectrum of a regular amorphous structure.

Nevertheless, it is possible to refine the original XRD spectrum with the aid of a mineral database. Hanawalt and Fink's searching method has been used to compare our results with the regular patterns produced and published by the Joint Committee for Powder Diffraction System (JCPDS). The spectra in the lower part of Figure 9 have been inserted from the literature and refer to the 32-171 and 18-996 materials, which are N-(2-Hydroxy-4-methoxybenzylidene)-p-propylaniline and Potassium-Calcium-Phosphate, respectively. The same lines are visible in the lignin spectrum part.

The decomposition lines of the lignin spectrum are compared to the lines of these two special materials spectra. Hydroxyls and other phases composed of potassium, calcium, and phosphorus are identified, indicating that these elements are also present in the lignin. In conclusion, our results characterize a tridimensional amorphous macro-molecule whose primary precursors contribute to the polymerization process of the final composite sample.

Attenuation of gamma radiation

The physical characterization of this composite is indeed important. Nevertheless, it is crucial to quantify the intensity of gamma radiation that this new material can effectively shield, especially in comparison to pure standard tungsten. In fact, this is the central question

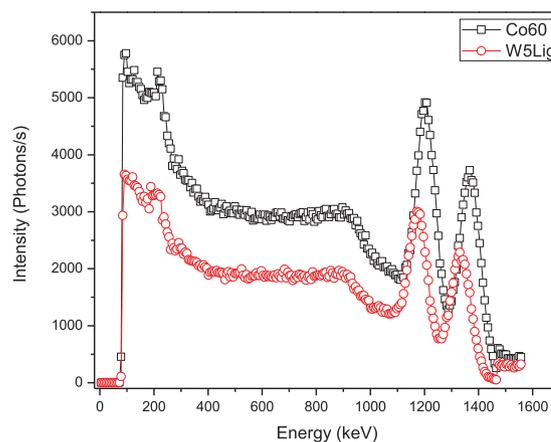


Figure 11. Intensity of gamma radiation reaching the detector for the free path (square symbols) and after passing the tungsten-lignin composite (circles).

concerning any possibilities of its application in equipment and devices to shield radiation.

A sample of Co-60 has been used as a source of controlled gamma radiation. The direct radiation has been measured to count the total number of emitted photons, i.e., the free intensity pointed to the meter.¹⁹ A second measurement has been realized, but this time with the composite placed between the source and the detector. The attenuation of the gamma radiation due to the presence of the composite is visible in Figure 11.

The graphic shows the emitted intensity, i.e., the number of photons per second of the gamma radiation source as a function of the photon energies, measured in keV. The dark boxes represent the amount of radiation that went directly from the source to the detector. The red circles represent the measurements of radiation passing through the composite before reaching the detector.

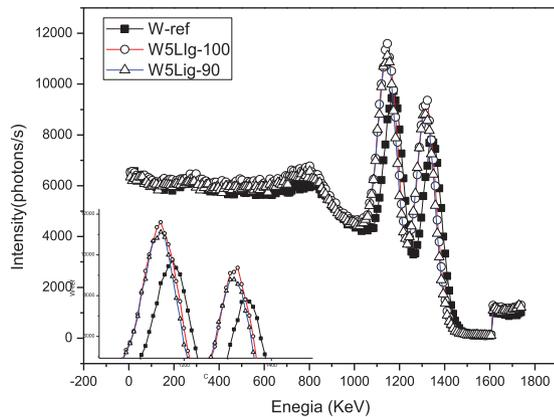


Figure 12. Gamma radiation intensity as a function of the photon energy measured after passing thru tungsten and two composites sintered at different temperatures.

The intensity presents two major peaks, which characterize the Co-60 sample. They are located at 1,173 keV and 1,332 keV, respectively. The intensity measured of the radiation having passed through the composite is smaller than the free beam, as expected. Only 61% of the original gamma radiation crossed the composite, i.e., 39% of the incident photons have been shielded by the W5Lig composite.

It is yet necessary to verify how effective this composite attenuates gamma radiation compared to standard tungsten. Important goals have been achieved until now. The new composite is malleable and still deviates a part of the incident gamma radiation. It can be molded and modified much easier than pure tungsten.

The final characterization is the measure of the attenuation coefficient of gamma radiation for the composite and tungsten. The first goal is a direct comparison of these values. In the sequence, measurements of the radiation intensities have been done in two different situations involving a composite inserted as a barrier to block the gamma radiation.

A secondary objective in this part is to study the effect of the composite sintering temperature on the attenuation coefficient. The present results compare two W5Lig samples sintered at 90 °C and 100 °C, respectively. It's already been concluded that these are the more efficient temperatures of sintering, as the agglutination is enhanced at these values. Every sample to be irradiated is positioned at the same distance between the gamma radiation source and the detector. The difference between these two series of measurements is the sintering temperature of each composite. Therefore, these two characteristic curves are directly comparable.

The experimental data are exhibited in Figure 12. The graphic shows the intensity of gamma radiation

as a function of the incident photon energy. Three characteristic curves are exhibited to be discussed. The first curve has dark-filled square symbols and represents the radiation intensity that passes through pure tungsten. The two other characteristic curves have empty symbols and refer to the W5Lig composite. Empty circles and triangles indicate the radiation intensity measured for the composites sintered at 100 °C and 90 °C, respectively.

In the magnified area, the major principal peaks are amplified. The intensity measured using the composites is higher than the intensity observed when pure tungsten is used, as expected. It goes for all the range of energy. The shielding effect of the pure tungsten is maximal in normal conditions. The lignin forming the composite certainly reduces the condition of attenuation for the mixed material. No relevant differences are noticed between the intensities of the composites sintered at 90 °C and 100 °C. Therefore, the analysis of the SEM micrographs together with the measurement of intensities leads to conclude that 90 °C is the optimal temperature for sintering the composite.

Therefore, this experiment serves to quantify the shielding effect of tungsten compared to a composite. The composite is formed with 5% lignin added to tungsten powder and sintered. It is essential to understand whether this new material can safely deviate incident gamma radiation. These results help to clarify how effective the composite shields radiation compared to pure tungsten.⁵

The numerical results obtained on these experiments are resumed in Table 2. The first column identifies the specific sample submitted to gamma radiation; the second column indicates the applied radiation intensity, which was constant for all measurements. The measurements of the transmitted intensity are shown in the third column; the calculated attenuation ratios are in the fourth column; The sample thicknesses are in the fifth column. The two last columns are filled with the calculated coefficient of attenuation and the mass densities of each related sample, respectively. It is important to point out that the distance separating the gamma source and the detector is kept constant, whether there was a sample in between or not.

The inclusion of 5% lignin to form the composite reduces the composite mass density to less than half the pure tungsten value. Therefore, the new composite is more than only malleable, as previously argued, but it is considerably lighter too.

The composite mass density sintered at 100 °C is slightly lighter than the equivalent for the composite sintered at 90 °C, as expected. However, other parameters related to the heating treatment at 90 °C, including the attenuation coefficient, indicate that the best sintering occurs at this temperature. The transmitted

Table 2. Results from the measurements of gamma radiation experiment.

Sample characteristic	Incident photons (I_0)	Transmitted photons (I_x)	Attenuation ratio $\ln(I_0/I_x)$	Thickness X (cm)	Attenuation coefficient μ (cm^{-1})	Density (gr/cm^3)
Standard tungsten	12620	9717	0.261	0.607	0.429	19.163
W5Lig $T_s = 100^\circ\text{C}$	12620	11594	0.084	0.644	0.130	8.241
W5Lig $T_s = 90^\circ\text{C}$	12620	11121	0.126	0.679	0.185	8.259

intensity of radiation and the attenuation coefficient, the agglutination process, and the surface morphology are all more appropriate in this case.

The degradation process of lignin is not evaluated in this paper. It remains a question to be analyzed in future studies. The used source of Co-60 presents a low radioactive activity on the order of 35 μCi , and the time of exposure has been limited to 30 minutes. According to Souza,²⁰ the degradation of cellulose and lignin demands absorption doses in the order of 11 kGy.

Conclusion

A new organic-metallic composite obtained from the sintering of Kraft lignin and tungsten is presented for the first time. Initially, the method to obtain the Kraft lignin is entirely described. Then, the procedure to mix and press lignin and tungsten powder is detailed. The technique of the heating treatment to form the composite is presented. Results obtained at different sintering temperatures are discussed, looking to determine the optimal conditions.

Physical characterizations of this composite have been performed, presented, and discussed in this paper. The surface of different samples is analyzed with the help of SEM micrographs. These results are crucial to understanding the resulting process of sintering. Complementary measurements using EDS are obtained to study the elements forming the composite. They are useful to study allowed electronic transitions in the composite. Measurements of XRD characterize the composite as an amorphous material presenting hydroxyls and other phases composed of potassium, calcium, and phosphorus. These structures and elements come from the lignin. It is always important to enhance the microscopic characterization of new materials. Studies using SEM exhibiting results in nanoscale for organic material such as, e.g., polymers and cellulose to obtain morphological and composition details of the sample are common. This is done by applying energies in the 2 to 5 keV range, typically. However, the sample described in this paper is not suitable for these measurements, as such radiations would imply the degradation of the lignin, which would compromise the results.

An experiment tested the shielding effect of this composite to retain gamma radiation and compared it to the properties of pure tungsten. Standard tungsten is known as an excellent material to shield gamma radiation. However, it is very dense and hard, turning its application difficult and resulting in heavyweight devices. The mixture uses 5% lignin and results in a composite whose mass density is smaller than half of the tungsten. Two useful features resulting from this new composite are malleability and density, particularly when compared to standard tungsten. The presence of lignin makes the composite easier to machine. The composite is lighter, malleable, free of oxidation, and homogenous, especially when sintered at 90°C .

Experimental results comparing the use of this composite and pure tungsten to shielding gamma radiation are discussed. The present results determine how the insertion of lignin modifies the advantages associated with tungsten regarding the shielding effect. The present paper shows that the attenuation due to the composite is only 16% smaller than the attenuation resulting from pure tungsten. Although 16% might seem a considerable value, the gains obtained from other aspects highly compensate for such a reduction. It is possible to improve the attenuation using a piece of material slightly thicker, which shall remain malleable and lighter yet. The new composite is promising regarding the fabrication of elements used as protection against damageable radiations.

Acknowledgements

One of us, FA, is grateful to the Brazilian National Council for Scientific and Technological Development, CNPq, for financial support.

Declaration of Conflicting Interests

The author(s) declared no potential conflicts of interest with respect to the research, authorship, and/or publication of this article.

Funding

The author(s) disclosed receipt of the following financial support for the research, authorship, and/or publication of this article: This study was supported by the Brazilian National Council for Scientific and Technological Development, CNPq (to FA).

ORCID iDFlavio Aristone  <https://orcid.org/0000-0003-3172-7520>**References**

1. Ehmman WD and Vance DE. *Radiochemistry and nuclear methods of analysis*. New York: John Wiley and Sons, 1991.
2. Lee JH, Hwang SK, Yasuda K, et al. Effect of molybdenum on electron radiation damage of Zr-base alloys. *J Nucl Mater* 2001; 289: 334–337.
3. Xiao WX, Jiancheng T, Nan Y, et al. Novel preparation method for W-Cu composite powders. *J Alloys Compd* 2016; 661: 471–475.
4. Chen LC and Ma SH. Effects of Ni/Co ratio and mechanical alloying on characteristics and sintering behavior of W-Ni-Co tungsten heavy alloys. *Journal of Alloys and Compounds* 2017; 711: 488–494.
5. Leroy C and Rancoita P. *Principles of radiation interaction in matter and detection*. Singapore: World Scientific, 2004.
6. Chen W, Dong L, Zhang H, et al. Microstructure characterization of W-Cu alloy sheets produced by high temperature and high-pressure deformation technique. *Mat Lett* 2017; 205: 198–201.
7. Zivelonghi A and You JH. Mechanism of plastic damage and fracture of a particulate tungsten-reinforced copper composite: a microstructure-based finite element study. *Comput. Mater Sci* 2014; 84: 318–326.
8. Kim J, Lee J, Park J, et al. Catalytic pyrolysis of lignin over HZSM-5 catalysts: effect of various parameters on the production of aromatic hydrocarbon. *J Anal Appl Pyrol* 2015; 114: 273–280.
9. Paiva JMF. *Compósitos LignoCelulósicos: Matrizes Poliméricas de Resinas Fenólicas Reforçadas com Fibras de Bagaço de Cana-de-Açúcar*. Dissertação (Mestrado), Instituto de Química de São Carlos, Universidade de São Paulo, São Carlos, Brazil, 1997, p. 94.
10. Carrott PJM and Ribeiro Carrott MML. Lignin—from natural adsorbent to activated carbon: a review. *Biores Tech* 2007; 98: 2301–2312.
11. Zakaryan M, Kirakosyan H, Aydinyan S, et al. Combustion synthesis of W-Cu composite powders from oxide precursors with various proportions of metals. *Int J Refract Metals Hard Mater* 2017; 64: 176–183.
12. William DE and Vance DE. *Radiochemistry and nuclear methods of analysis*. New York: John Wiley and Sons, 1991, pp. 162–175.
13. Fergus BJ and Goring DAI. The distribution of lignin in birch wood as determined by ultraviolet microscopy. *Holzforchung* 1970; 24: 118–124.
14. Haessner F. Systematic survey and basic problems of recrystallization. In: Haessener F (ed.) *Recrystallization of metallic materials*. Stuttgart: Dr. Riederer Verlag, 1978, pp. 1–3.
15. Asada C, Basnet S, Otsuka M, et al. Epoxy resinsynthesis using low molecular weight lignin separated from variouslignocellulosic materials. *Int J Biol Macromol* 2015; 74: 413–419.
16. Brebu M, Tamminen T and Spiridon I. Thermal degradation of various lignins by TG-MS/FTIR and Py-GC-MS. *J Anal Appl Pyrol* 2013; 104: 531–539.
17. Liu C, Hu J, Zhang H, et al. Thermal conversion of lignin to phenols: relevance between chemical structure and pyrolysis behaviors. *Fuel* 2016; 182: 864–870.
18. Lawoko M, Henriksson G and Gellerstedt G. Structural differences between the lignin-carbohydrate complexes present in wood and in chemical pulps. *Biomacromolecules* 2005; 6: 3467–3473.
19. Nelson G and Reilly D. Gamma-ray interactions with matter. In *Passive nondestructive analysis of nuclear materials*. Santa Fe: Los Alamos National Laboratory, NUREG/CR-5550, LA-UR-90-732, 1991, pp. 27–42.
20. Souza ACD, Cione FC and Silva ACD. Evaluation of a metal-organic composite (tungsten-lignin) for attenuation of gamma radiation. *Mat Res* 2019; 22, p: 1–5, dx. doi.org/10.1590/1980-5373-mr-2019-0045.